Theoretical Study on the Structural Properties and Relative Stability of M(II)−Al Layered Double Hydroxides Based on a Cluster Model

Hong Yan,[†] Min Wei,*[,†] Jing Ma,[‡] Feng Li,[†] David G. Evans,[†] and Xue Duan[†]

State Key Laboratory of Chemical Resource Engineering, Beijing University of Chemical Technology, Beijing 100029, P. R. China, and Institute of Theoretical and Computational Chemistry, Key Laboratory of Mesoscopic Chemistry of MOE, Nanjing University, Nanjing 210093, P. R. China

Received: November 18, 2008; Revised Manuscript Received: April 6, 2009

The $[M_2Al(OH_2)_9(OH)_4]^{3+}$ clusters (M = divalent cation Mg^{2+}, Ca^{2+}, Mn^{2+}, Fe^{2+}, Co^{2+}, Ni^{2+}, Cu^{2+}, Zn^{2+}, or Cd^{2+}), which include the basic information of layered double hydroxides (LDHs) lattice structure with the most economical size, have been investigated by density functional theory (DFT) to shed light on the structural properties and relative stability of M(II)−Al binary LDHs layers with a M^{2+}/Al^{3+} ratio of 2. The geometric parameters (bond distance and bond angle), natural bond orbitals (NBO), stretching vibration frequencies of three-centered bridging OH groups (ν(O3-H)), as well as binding energy of the cluster model were systematically studied. It was found that the geometries and the ν(O3-H) frequency for the calculated clusters are remarkably influenced by the electronic structure of the divalent cations, such as valence electronic configuration, natural bond orbitals, natural charge transfer, and bond order. The calculated binding energies are in good agreement with the relative stability of the experimental results for the corresponding LDHs. The calculation results reveal that the 2Ni−Al cluster shows the highest stability among the open-shelled cation-containing clusters, while the stability of the 2Cu−Al cluster is the weakest; the 2Mg−Al and 2Zn−Al clusters are the most stable ones among the closed-shelled cation-containing clusters. These findings are in high accordance with the experimental results. Therefore, this work provides a detailed understanding of how the electronic structure of cations plays a more significant role in the structural properties and relative stability of the corresponding LDHs layers rather than ionic size.

Introduction

Layered double hydroxides (LDHs), also called anionic clay and hydrotalcite-like compounds, are host−guest layered materials with the general formula $[M^{2+}_{1-x}M^{3+}_{x}(OH)_2]^{x+}(A^{n-}_{x/n})\cdot mH_2O$, where M^{2+} and M^{3+} are metal cations that occupy octahedral positions in hydroxide layers; x is the molar ratio $M^{3+}/(M^{2+} + M^{3+})$; and A denotes interlayer charge-compensating anions.[1−4] A wide range of LDHs containing various combinations of M^{2+}, M^{3+}, and A^{n-} ions have been synthesized. Observed M^{2+} and M^{3+} species include Mg^{2+}, Ni^{2+}, Co^{2+}, Mn^{2+}, Cu^{2+}, Cd^{2+}, Ca^{2+}, Fe^{2+}, Zn^{2+}, etc. and Al^{3+}, Ga^{3+}, Fe^{3+}, Cr^{3+}, etc., respectively.[3,4] Furthermore, LDHs containing more than two species of cations have been prepared.[5] Besides the common $M^{2+}-M^{3+}$ LDHs, the $M^{+}-M^{3+}$ LDHs (Li−Al LDH is the only known example)[6] and $M^{2+}-M^{4+}$ (e.g., Ti^{4+}, Zr^{4+}, or Sn^{4+}) LDHs[7a−c] were also reported, although doubt has been cast on the Zr^{4+}- or Sn^{4+}-containing LDHs.[7d] The versatile availability in chemical composition allows LDH materials with a wide variety of physiochemical properties. Recently, the lamellar structure and the anion-exchange properties of LDHs make them attractive for both fundamental investigations and technological applications in the fields of catalysis,[8a] gene and molecular reservoir,[8b] optical materials,[8c] functional hybrid nanostructured materials,[8d] controlled drug-release system,[8e] and thin films.[8f−i]

Empirically, cations with an ionic radius not too different from that of Mg^{2+} (0.72 Å)[9] can be accommodated in the center of the close-packed OH groups in the brucite-like layers to form LDH materials. Nevertheless, there are still some discrepancies which have not been understood thoroughly. The most apparent examples are the cases of Ni^{2+} and Cu^{2+}. They have very close ionic radii (0.69 and 0.73 Å, respectively) to that of Mg^{2+}; however, Ni^{2+} is easy to be introduced into LDH layers, and the Ni^{2+}-containing LDHs have widely been studied,[10] whereas the Cu^{2+}-containing LDHs show a corrugation of the sheets or should be diluted by other divalent cations.[11] This is generally explained by Jahn−Teller distortion, but the more detailed structural information of LDH materials is limited, due to the difficulty in probing the hydroxide matrix structure based on experimental techniques.

With recent advances in computational software and hardware, theoretical calculations are now able to extend the scope of study of these materials beyond experimental observations. A number of force-field based simulations[12] and quantum chemical calculations[13−15] were reported on the modeling of LDHs to study some specific properties related to the interlayer anions and the electronic structure inside LDH host layers.

In our previous work, a series of octahedral hexadydrated metal cations have been studied by the density functional theory method for the understanding of their template effects on the construction of LDH layers.[16] Whether a cation can be introduced into an LDH layer stably has been discussed. The present work was carried out to provide further understanding of the structural properties and relative stability of LDH layers containing different divalent cations. Since the structure of the octahedra sheets of LDHs is dependent on a local environment, the choice of a practical cluster model is a good approach for the study. In the present work, a cluster model

* Corresponding author. Phone: +86-10-64412131. Fax: +86-10-64425385. E-mail: weimin@mail.buct.edu.cn.
[†] Beijing University of Chemical Technology.
[‡] Nanjing University.

10.1021/jp810129h CCC: $40.75
Published on Web 05/01/2009

of the LDH layer containing three cations presented by the formula $[M_2Al(OH_2)_9(OH)_4]^{3+}$ was proposed since it includes the basic information of the lattice structure of LDHs with the most economical size. A series of $[M_2Al(OH_2)_9(OH)_4]^{3+}$ clusters (M = Mg^{2+}, Ca^{2+}, Mn^{2+}, Fe^{2+}, Co^{2+}, Ni^{2+}, Cu^{2+}, Zn^{2+}, or Cd^{2+}), containing Al^{3+} and the most commonly reported divalent cations, have been studied by the density functional theory method. Herein, the geometric parameters (bond distances and bond angles), stretching vibration frequencies of three-centered bridging OH groups, and binding energy of the cluster model were systematically discussed. Furthermore, the valence electronic configurations of metal ions and Jahn−Teller effects, which influence the structure of LDH sheets, have also been studied. Natural bond orbital (NBO) analyses have been applied to examine in detail the nature of M−O bonding and the relationship between the M−O bonding and relative stability of LDHs. It was found that the electronic structure of the divalent cations plays a more significant role in the structural properties and relative stability of the LDH layers rather than the ion size. The results of theoretical calculation in this work are in high accordance with the experimental findings.

Computational Details

Cluster Model of LDH Layers. To carry out the theoretical study, it is necessary to choose an economical cluster model which includes the basic information. According to our previous study,[16] the $[Mg_3(OH_2)_9(OH)_4]^{2+}$ cluster containing three Mg^{2+} cations is stable and thus proposed to be the most practical model for the brucite-type layer.

On the basis of the intimate structural relationship between LDHs and brucite, a cluster model containing three metal cations was also used to carry out the calculation for the brucite-like layer of LDHs in this work. It is known that the maximum substitution of Al^{3+} ions in a Mg^{2+} hydroxide layer corresponds to a Mg:Al ratio of 2:1,[1,3] and any larger substitution of Al^{3+} in adjacent octahedral centers may thereby lead to nucleation of an $Al(OH)_3$ phase. As a result, we use the cluster formulated as $[M_2Al(OH_2)_9(OH)_4]^{3+}$ (M = Mg^{2+}, Ca^{2+}, Mn^{2+}, Fe^{2+}, Co^{2+}, Ni^{2+}, Cu^{2+}, Zn^{2+}, and Cd^{2+}), which contains two divalent cations and one trivalent cation, to study the structural properties of M(II)−Al binary LDH layers with a M^{2+}/Al^{3+} ratio of 2. This is in accordance with the fact that all the hydroxides of the above divalent cations or at least one modification of each hydroxide crystallize in layered brucite-type lattices.[17]

In this model, each bridging oxygen atom in M−O−M and Al−O−Al is set to be bonded to one hydrogen atom (OH group), and the terminal oxygen atoms are set to be bonded to two hydrogen atoms (OH_2 group), in avoidance of the appearance of the unpaired electrons in the truncated ligands. Thus, as displayed in Figure 1A, the model has one OH group at the three-centered bridging position, three OH groups at the two-centered bridging position, and nine OH_2 groups at terminal edges. It has been proven by Sato et al. that the presence of the three-centered bridging OH group is essential to stabilize a cluster for creating a layered structure.[15c] This also agrees with the structure of the LDH crystal lattice in which each hydroxyl group is bonded to three cations.

The transition cations with open-shelled configuration such as Mn^{2+}, Fe^{2+}, Co^{2+}, Ni^{2+}, and Cu^{2+} are calculated only in the high-spin state since they are coordinated with the weak field ligands (OH groups and OH_2 groups)[18] in the LDH lattice.

Density Functional Calculations. Theoretical calculations were carried out on the $[M_2Al(OH_2)_9(OH)_4]^{3+}$ (M = divalent metal cation) clusters. The geometrical optimization for the cluster model was performed by the density functional theory (DFT) with the three-parameter hybrid functional (B3LYP).[19] The effective core potential (ECP), LANL2DZ,[20] is employed to the divalent metal ions, and the full electron basis sets, 6-31G(d),[21] are used for Al, O, and H, respectively. Mg and Ca were also treated with 6-31G(d) basis sets besides LANL2DZ ones. It was found that the calculation results by the two basis sets are close to each other for the 2Mg−Al and 2Ca−Al clusters (Table 1), verifying that the use of the LANL2DZ basis sets is reliable. The calculations were performed with the Gaussian 03 program suite.[22]

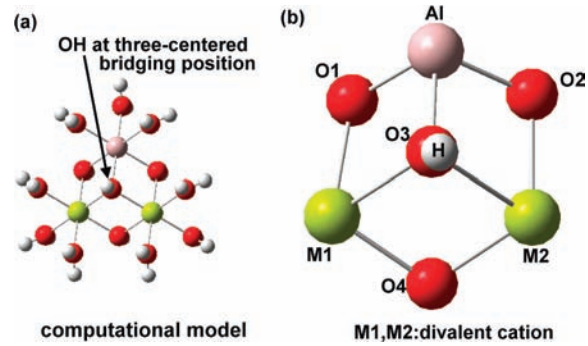

Figure 1. (A) Computational model of $[M_2Al(OH_2)_9(OH)_4]^{3+}$ (M = divalent metal cation) clusters. (B) One part of the cluster model including the linkage around the three-centered bridging OH group which is used to analyze the calculation data.

No constraints were imposed on the geometry in any of the computations. The attainment of the energy minimum of each structure in full geometry optimization was tested by frequency calculations. The reported energies in this work were corrected by zero-point energy (ZPE). The B3LYP/6-31G(d) scale factor (0.9603) was applied to the calculated vibrational frequencies due to a deficiency of the theory (such as an inadequate basis set or neglect of correlation) as well as the anharmonicity of the potential.[23]

Natural Bond Orbital Analysis. Natural bond orbital (NBO) analysis has been demonstrated as a useful tool to provide a quantitative description of interatomic and intermolecular interactions in accordance with the classical Lewis structure concepts.[24] In the present work, we use NBO analysis to describe the charge distributions and the bonding interactions between the metal ions and three-centered OH ligand in the $[M_2Al(OH_2)_9(OH)_4]^{3+}$ model. The natural localized molecular orbitals/natural population analysis (NLMO/NPA) was also performed to indicate the strength of the M−O bond.

NBO analysis was carried out at the UB3LYP/LANL2DZ/6-31G(d) level using the NBO 5.0 program and built-in NBO 3.1[25] subroutines of the Gaussian 03 program.

Results and Discussion

Geometry and Electronic Configuration. The optimized structures of the $[M_2Al(OH_2)_9(OH)_4]^{3+}$ clusters display different geometries with C1 symmetry, as shown in Figure S1 (Supporting Information). In the following discussion, we concentrate on the part of the cluster which is linked around the OH group at the three-centered bridging position (Figure 1B). The optimized geometries of the calculated clusters such as average interatomic distance, bond lengths, and bond angles are listed in Table 1, along with the experimental data.

It can be seen from Figure S1 (Supporting Information) that the general geometry of these calculated clusters is close to that of the octahedral layer of LDHs. Both the local geometry around

TABLE 1: Optimized Geometries of $[M_2Al(OH_2)_9(OH)_4]^{3+}$ (M = Divalent Metal Cation) Clusters along with the Experimental Results (The Atomic Labels Are Shown in Figure 1B)

(A) Effective Ionic Radii *r* (in Å)[9] for Divalent Cations in 6-Fold Coordination, Bond Lengths (in Å), and Interatomic Distances (in Å)

		M−O		Al−O3	M1···M2		M···Al		O3−H
M	*r*	calcd[a]	exptl	calcd	calcd	exptl	calcd[e]	exptl	
Mg ($3s^0$)	0.720	2.191	1.974−2.123[26a]	1.885	3.139	3.046[26b]	3.037	1.979−2.097[26a]	0.968
		2.202[b]	2.013[26b]	1.884[b]	3.150[b]	3.142[c,26c]	3.042[b]	1.900−1.910[c,26o]	0.968[b]
			2.102[c,26c]						
Ca ($3d^04s^0$)	1.000	2.505	2.344−2.474[26d]	1.877	3.743	3.583[c,26e]	3.366	1.903−1.918[26d]	0.969
		2.510[b]	2.363[c,26e]	1.874[b]	3.774[b]		3.365[b]		0.968[b]
Mn ($3d^5$)	0.830	2.279	2.196[c,26f]	1.891	3.315	3.322[c,26f]	3.1175		0.969
Fe ($3d^6$)	0.780	2.227	1.955[d,26g]	1.888	3.234	3.262[c,14]	3.0705		0.969
Co ($3d^7$)	0.745	2.229	2.070−2.100[26h]	1.882	3.158	3.080−3.120[26h]	3.055		0.969
			2.097[c,26i]			3.173[c,26i]			
Ni ($3d^8$)	0.690	2.118	2.136[c,26j]	1.915	3.129	3.114[c,26j]	2.987		0.970
Cu ($3d^9$)	0.730	2.241	1.948−1.972[c,26k]	1.894	3.214	2.947[26k]	3.033		0.971
Zn ($3d^{10}$)	0.740	2.301	2.268[c,26l]	1.854	3.171	3.085[26m]	3.105		0.967
						3.194[c,26l]			
Cd ($4d^{10}$)	0.950	2.463	2.315[c,26n]	1.858	3.490	3.496[c,26n]	3.282		0.967

(B) Bond Angles (in degree)

	O−M−O		O−Al−O	
M	calcd[f]	exptl	calcd[g]	exptl
Mg	76.81	81.67[26b]	86.36	
	76.70[b]	83.30[c,26c]	86.56[b]	
Ca	71.85	64.66−117.45[26d]	90.34	95.09−95.42[26d]
	71.81[b]	90.54[c,26e]	90.43[b]	
Mn	72.42	81.72[c,26f]	88.99	
Fe	75.52		87.25	
Co	76.14	81.68[c,26i]	85.83	
Ni	78.14	86.43[c,26j]	88.44	
Cu	77.92	81.97[c,26k]	85.82	
Zn	75.10	86.43[c,26l]	86.39	
Cd	72.42	81.92[c,26n]	88.99	

[a] Average value of M1−O3 and M2−O3 (Figure 1B). [b] All-electron 6-31G(d) basis sets. [c] Data of metal hydroxide. [d] Data of iron fluoride tetrahydrate. [e] Average value of M1···Al and M2···Al. [f] Average value of O1−M1−O3, O4−M1−O3, O2−M2−O3, and O4−M2−O3. [g] Average value of O1−Al−O3 and O2−Al−O3.

the metal and the close packing of the hydroxyl anions are significantly distorted away from their idealized arrangements, which leads to the increase in the O···O and M···M distance from those of the ideal O_h geometry, with the O−M−O bond angle distorted considerably (typically by 7−8°) rather than a regular 90°. Each M−O3 (atomic label shown in Figure 1B, the same in the following text) bond length and O−M−O bond angle of all the calculated clusters show a very close value except for the 2Cu−Al cluster which exhibits the most serious distortion. This is related to the well-known tendency for Cu^{2+} to occupy octahedral coordination with a strong tetragonal (4 + 2)-distortion, usually explained in terms of a static Jahn−Teller effect.[18]

As shown in Table 1, in general, good accordance was found between the theoretically calculated M−O or Al−O3 bond length and the experimental value. In most cases, calculated M−O bond lengths and M···M interatomic distances are slightly longer than the experimental ones except for the case of the 2Cu−Al cluster, while the Al−O3 bond lengths are slightly shorter than the experimental values. This is because the experimental values derive from LDHs or metal hydroxide crystal data, in which the interaction between adjacent layers does exist. However, the calculated cluster only presents the basic information of a single layer. In the exception case of the 2Cu−Al cluster, serious discrepancy was found between the calculated bond length and the experimental one. This is due to the large distortions in the calculated geometry as well as the experimental data which come from the specific lattice of copper hydroxide. In fact, the copper hydroxide forms a different lattice from brucite but closely related to the structure of γ-FeOOH.[26k] Only small differences are found for the O−H bond length of these clusters. In the 2Mg−Al cluster, the calculated O−H bond length (0.968 Å) is very close to the experimental value for brucite (0.958 Å),[27] and the calculated values of Mg−O, Al−O3, and O−H (2.191, 1.885, and 0.968 Å, respectively) are very close to those obtained previously from the periodic ab initio method in ref 13b (2.193, 1.890, and 0.969 Å, respectively). This demonstrates that the cluster model in this work gives comparable results to those of the periodic ab initio method. On the other hand, all the average O−M−O and O−Al−O angles in the calculated clusters are smaller than the experimental values, due to the absence of the interaction between adjacent LDH layers.

The bond length, interatomic distance, or bond angle of $[M_2Al(OH_2)_9(OH)_4]^{3+}$ clusters as a function of the atomic number of M^{2+} are shown in Figure 2. The closed-shelled cations and the open-shelled ones are linked by dashes. As shown in Figure 2A and 2B, the bond lengths, interatomic distances, and bond angles related to the closed-shelled divalent cations (Mg^{2+}, Ca^{2+}, Zn^{2+}, Cd^{2+}) in the clusters monotonically increase from Mg^{2+} to Ca^{2+} and from Zn^{2+} to Cd^{2+} with the increase of the period number, respectively. On the contrary, both the Al−O3 length and O−Al−O angle decrease with the increase of the period number, due to the smaller ionic radius

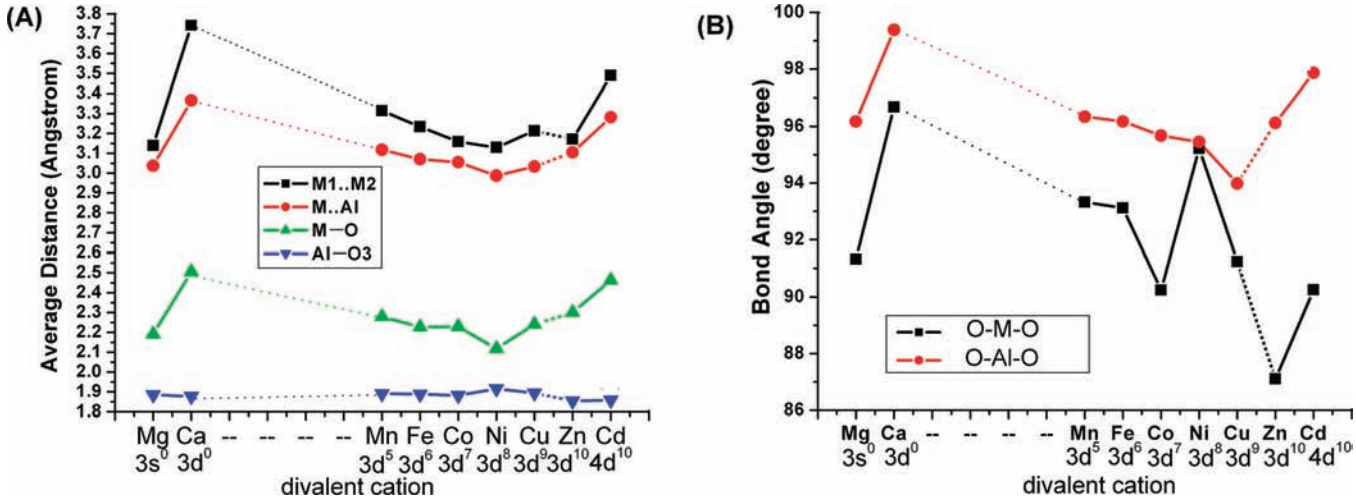

Figure 2. (A) Bond length, interatomic distance, and (B) bond angle of $[M_2Al(OH_2)_9(OH)_4]^{3+}$ (M = divalent metal cation) clusters as a function of atomic number of M^{2+}. The atomic labels are shown in Figure 1B. M−O is the average value of M1−O3 and M2−O3; M···Al is the average value of M1···Al and M2···Al; O−M−O is the average value of O1−M1−O3, O4−M1−O3, O2−M2−O3, and O4−M2−O3; O−Al−O is the average value of O1−Al−O3 and O2−Al−O3.

of Al^{3+} (0.535 Å) than that of the divalent cations. However, in the case of the clusters including the open-shelled transition divalent cations from Mn^{2+} to Cu^{2+}, the changes of the bond length, interatomic distance, and bond angle are not monotonic. The tendencies of the distances of M1···M2, M···Al, and M−O length are similar to that of the ionic radius of these transition cations,[18] reaching a minimum at Ni^{2+}. This is related closely to their electronic configuration. Since in the crystal-field model, the d^8 electrons of Ni^{2+} occupy all the t_{2g} state, leading to a minimum of the radius. The radius for d^9 of Cu^{2+} is, however, larger than that of d^8 because the additional electron occupies the e_g state. This ligand field effect results in the similar changes in the calculated distances of M1···M2, M···Al, and M−O length which are related to the ionic radius of the corresponding divalent cations. Actually, the unit cell volume of the different hydroxides from Ca to Zn as a function of their respective number of 3d-electron also shows the similar tendency.[17] The resulting diagram reflects the expectations satisfactorily by taking into account the ligand field stabilization energies (LFSEs) for octahedral coordinated high-spin ions.[18] However, the Al−O3 length and O−M−O angle display the opposite tendency to that of the ionic radius, reaching a maximum at Ni^{2+}. For the O−Al−O bond angle, although it decreases from Mn^{2+} to Co^{2+}, it also reaches a maximum at Ni^{2+}. This result reveals that the 2Ni−Al cluster possesses the most stable geometry, which agrees well with the experimental fact that Ni^{2+} is much easier to be introduced into the LDH layers than the other transition cations.[10]

On the basis of the discussion above, it can be concluded that different electron configurations of the divalent cations lead to different geometries of the calculated clusters containing the corresponding cations and also result in a significant influence on the structural properties of the LDH layers.

Natural Bond Orbital Analysis. The NBO analysis provides information about the Lewis and the non-Lewis (Rydberg) structure.[28] The analyses of the individual electron densities were carried out separately for α (spin-up) and β (spin-down) orientations for the open-shelled systems, reflecting the two different opportunities by which a single electron can occupy a metal orbital in terms of the spin direction.[24]

In all studied clusters, the interaction between the divalent metal atom and the oxygen atom is to be considered as an electronic delocalization from O hybrid orbitals containing s character and p character to metal pure $(n + 1)$s or d orbitals. On the other hand, formal Al−O3 and O3−H bonding orbitals exist in these studied systems, and the most significant interaction is the delocalization from the Al−O3 σ-bonding orbital to the Al−O3 σ-antibonding orbital.

The percentages of the "natural Lewis structure" NLMO/NPA bond orders between metal cation and the three-centered bridging oxygen atom (O3) as well as those of between the O3 atom and the hydrogen atom (H) are listed in Table S1A (Supporting Information) and plotted in Figure 3. All the clusters present more than 98% natural Lewis structure (Figure 3A), suggesting the dominance of the Lewis-type component of the bonding. The clusters including closed-shelled main-group cations (Mg^{2+}, Ca^{2+}) show a stronger Lewis-type bond (>99.20%) than those of the clusters including closed-shelled transition cations (Zn^{2+}, Cd^{2+}) (>99.03% for both α and β spin) and open-shelled transition cations (Mn^{2+}, Fe^{2+}, Co^{2+}, Ni^{2+}, Cu^{2+}) (98.60 ∼ 99.60% for α spin and 98.30 ∼ 98.70% for β spin, respectively). In both α and β spin states for the open-shelled cations, the Lewis-type bond component in the studied $[M_2Al(OH_2)_9(OH)_4]^{3+}$ clusters was found to reach a minimum at M = Cu and a maximum at M = Ni, implying the strongest Lewis-type bond in the 2Ni−Al cluster and the weakest one in the 2Cu−Al cluster. This accounts for the referred fact above that the Ni−Al−LDH is quite easy to be synthesized, while the Cu−Al−LDH is not.

The natural localized molecular orbitals/natural population analysis (NLMO/NPA) bond orders[24] in Table S1A (Supporting Information) indicate the interaction of the M−O3, Al−O3, and O3−H bonding. It is well-known that the larger the bond order is, the stronger the bond strength is. As shown in Figure 3B, the clusters including closed-shelled cations represent the very close bond orders between M1−O3 and M2−O3, indicating the close strength of each M−O3 bond. It can be expected that distortion will occur if the bond strength of M1−O3 and M2−O3 shows different values. Therefore, the exhibition of the different M−O3 bond orders in the 2Cu−Al cluster implies its Jahn−Teller distorted geometry. By comparing Figure 2A with Figure 3B, it can be found that the shorter bond length results in the stronger bond order. Therefore, the strongest and the weakest M−O3 bond orders exist in the 2M−Al cluster

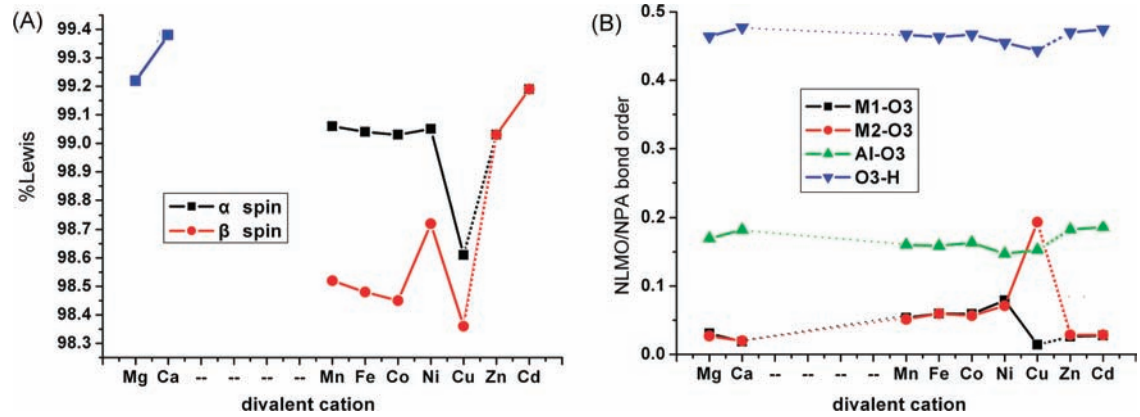

Figure 3. (A) Percentage of the "Natural Lewis Structure" and (B) NLMO/NPA bond orders between metal cation and the three-centered oxygen atom in $[M_2Al(OH_2)_9(OH)_4]^{3+}$ clusters as a function of the atomic number of M^{2+}.

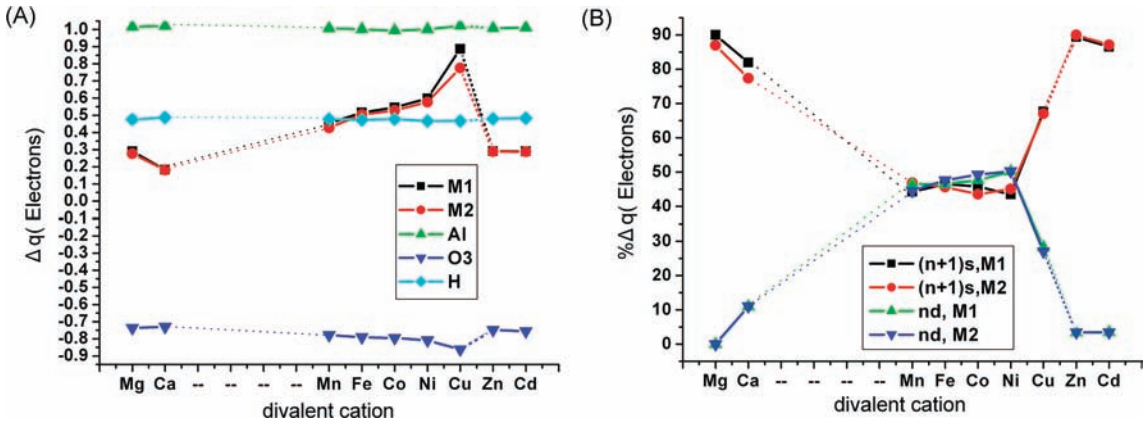

Figure 4. (A) Charge transfer (Δq) of metal cations and O, H ions and (B) the component of the charge transfer of $[M_2Al(OH_2)_9(OH)_4]^{3+}$ (M = divalent metal cation) clusters as a function of the atomic number of M^{2+}.

when M = Ni and Cu, respectively. This also indicates the stabilities of these two clusters and agrees with the experimental results of LDHs referred above.

The contributions of *n*d interaction and (*n*+1)s σ-interaction to natural charge transfer in the calculated clusters in electrons are reported in Table S1B (Supporting Information) and Figure 4. The calculated natural population analysis (NPA) for these clusters shows that there is a net transfer of electron density from each of the O ligands to the metal ions (Table S1B, Supporting Information). The transfer of electron density shows no remarkable variation for Al and H atoms but displays an obvious change for different divalent cations, suggesting that the electronic structure of the divalent cations imposes significant influence on the structural properties of the studied clusters. The charge transfer of the closed-shelled divalent cations decreases with the increase of the period number (Figure 4A; Table S1B, Supporting Information). The decrease from Mg to Ca (from 0.289e to 0.183e) is more significant than that from Zn to Cd (from 0.291e to 0.289e). However, in the case of the open-shelled cations, the transfer of density increases from M = Mn to Cu (from 0.452e to 0.887e for M1). The increase is not significant from M = Mn to Ni (from 0.452e to 0.598e) but quite remarkable from Ni to Cu (from 0.598e to 0.887e), implying a non-negligible covalent character of the metal−OH bonds in the 2Cu−Al cluster which is not obvious in the other clusters. On the other hand, since the electron density is transferred from the OH ligands to each metal cation, it leads to the change in the natural charge of the OH ligand and thus affects its bond strength, as shown by the smallest natural charge of the oxygen atom and O3−H bond order for the 2Cu−Al cluster in Figure 3B and Figure 4A, respectively.

The electron density shifted from the oxygen donor lone pairs (LPs) to the metal ions was judged by means of occupation numbers of the formally unoccupied *n*d and (*n*+1)s orbitals on the NBO basis. Applications of this method in the analysis of electronic structure of 3d $[M(H_2O)_6]^{3+}$ ions have been reported recently.[29] As can be seen in Table S1B (Supporting Information), the total charge transfer obtained in this way is virtually identical to the occupancy of *n*d and (*n*+1)s orbitals of natural electron configuration obtained via natural population analysis (NPA). This agreement shows the delocalization of metal electrons into empty antibonding orbitals of the ligands, and *n*p metal orbitals do not contribute significantly to the M−OH interaction in these cases. In addition, the clusters including closed-shelled cations show strong σ-interaction (>77.00%) and weak d interaction (<12.00%); the clusters including open-shelled cations exhibit close σ-interaction and d interaction (both about 43.00 ∼ 51.00%) except for the 2Cu−Al cluster with much stronger σ-interaction (∼67.00%) than d interaction (∼27.50%). Figure 4B reveals that σ-interaction becomes weaker, whereas d interaction turns stronger with the increase of the period number for the clusters including closed-shelled cations. However, in the case of the open-shelled cation-containing clusters, an inflection is found at M = Ni for each curve in Figure 4B, suggesting the strongest or weakest d interaction in the 2Ni−Al or 2Cu−Al cluster, respectively. From this point of view, the 2Ni−Al cluster possesses the strongest stability among the open-shelled cation-containing clusters, while the stability of the 2Cu−Al cluster is the weakest. This is also in accordance with the result obtained above and in good agreement with the experimental findings for LDHs.

TABLE 2: Scaled Stretching Vibration Frequencies of the Three-Centered Bridging OH Group ν(O3−H) (in cm^{-1}) and Zero-Point Corrected Binding Energies (ZPE) ΔE_b (in kcal·mol^{-1}) for the Optimized $[M_2Al(OH_2)_9(OH)_4]^{3+}$ Clusters, along with the Experimental Results

	ν(O3−H)		
M	calcd[a]	exptl	ΔE_b
Mg	3657 (83)	3500[30a]	3972.20
	3659 (83)[b]	3689[c,30b]	
Ca	3649 (52)	3400−3600[30c]	3708.45
	3650 (28)[b]	3640−3644[c,30b]	3784.47[b]
Mn	3646 (167)	2800−3600[30d]	3930.69
Fe	3643 (109)	3628[c,30b]	3981.58
Co	3642 (87)	3500[30e]	4027.64
		3629, 3624[c,30b]	
Ni	3628 (110)	3460[30f]	4040.50
		3620−3650[c,30b]	
Cu	3618 (75)	3300−3600[30g]	4054.08
Zn	3670 (113)	3440−3470[30h]	3991.86
Cd	3660 (160)	∼3400[30i]	3891.39
		3605−3620[30b]	

[a] Intensity values in brackets. [b] All-electron 6-31G(d) basis sets. [c] Data of metal hydroxide.

Stretching Vibration of the Three-Centered Bridging OH Groups. The hydroxyl groups play a major role in the catalytic activity of LDHs materials. In our cluster model, there is one OH group at the three-centered bridging position (O3-H, Figure 1B) which agrees with the lattice of LDHs. Therefore, the vibrational properties of these OH groups depend on the nature of the cations attached directly to them.[15d] The calculated scaled frequencies (by the scale factor 0.9603)[23] and relative intensities of the stretching vibrations for the O3−H group (ν(O3−H)) in the clusters are tabulated in Table 2 along with experimental data.

It can be seen from Table 2 that the scaled ν(O3−H) bands of the computation clusters appear at slightly higher frequencies than those of experiments. This can be explained by the existence of a hydrogen bond in the LDHs structure between the bridging OH group and interlayer anion or water molecule,[1] which is not involved in our computational model. Furthermore, the calculated ν(O3−H) values are much closer to those of the divalent hydroxides than to those of LDHs, due to the absence of a hydrogen bond in the divalent hydroxides such as $Mg(OH)_2$, $Ni(OH)_2$, etc.[17]

It is known that the ν(O3−H) frequency depends on the O3−H bond strength (k_{OH}) and the reduced mass of the vibration system (μ)[30b,31]

$$\nu = \frac{1}{2\pi c}\sqrt{\frac{k_{OH}}{\mu_{OH}}} \quad (1)$$

It can be seen from Table 2 that in the case of either closed-shelled cation-containing clusters or open-shelled cation-containing ones, the ν(O3−H) value decreases with the increase of atomic number from M = Mg to Ca and from Zn to Cd or from M = Mn to Cu. The results clearly show the dependence of ν(O3−H) on the mass of the associated cations that the more the mass sum of the system is, the less the ν(O3−H) value is. However, it is beyond expectation that the ν(O3−H) values of the 2Zn−Al and 2Cd−Al cluster become much larger (3670 cm^{-1} for Zn and 3660 cm^{-1} for Cd) than that of the 2Cu−Al cluster (3618 cm^{-1}), although the decline tendency exists from Zn to Cd. This fact is probably attributed to the different spin states between Zn, Cd, and other studied divalent transition cations in the calculation.

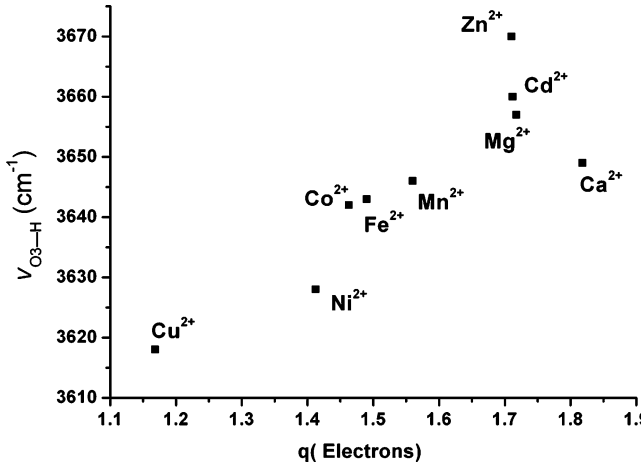

Figure 5. Scaled stretching vibration frequency of the three-centered bridging OH group (ν(O3−H)) in the cluster model plotted against the natural charge of the divalent cations by natural population analysis (NPA).

Vedder has correlated the k value with the valence of cations bonded to OH groups[31] because the O−H bond will be stronger by decreasing the common charge for both atoms. Accordingly, the ν(O3−H) frequency would decrease upon increasing the sum of valence of the corresponding cations. However, the opposite effect has also been reported.[32] Herein both the NPA natural charge of the divalent cations (Table S1B, Supporting Information) and the NLMO/NPA bond order of O3−H bond, which indicate the atomic valence and O3−H bond strength, respectively, were used to investigate the effect of the k value on the ν(O3−H) frequency. It was found in this work that the Vedder's model is applicable to some extent, in consistent with ref 33. For the closed-shelled cation-containing clusters, the ν(O3−H) frequency increases with the decrease of natural charges of the divalent cations, in good agreement with Vedder's model. However, the opposite tendency was found in the case of the open-shelled cation-containing clusters (see Figure 5). Comparing Figure 4A with Figure 3B, it can be seen that for the open-shelled cation-containing clusters the decrease in natural charge of the divalent cations leads to the augment of the charge transfer for the O3 atom and thus results in the weaker O3−H bond (smaller k value) and lower ν(O3−H) frequency. This might be due to the fact that Vedder's model follows the classical concept of the valence corresponding to ionic solids. However, for LDH materials, the bonds are not completely ionic but polarized covalent, which can be clearly explained by the percentage of the natural Lewis structure in Figure 3A. The clusters including closed-shelled cations show a stronger Lewis-type bond than that of clusters including open-shelled transition cations, suggesting the more ionic property of the former than the latter. Therefore, only the correlation between the ν(O3−H) frequency in the closed-shelled cation-containing clusters and the natural charges of divalent cations obeys Vedder's model.

In summary, the ν(O3−H) frequency is influenced by both the mass sum and the natural charge of divalent cations in the cluster. The mass sum plays a more significant role in determining the ν(O3−H) frequency for the clusters including closed-shelled cations. In the cases of the open-shelled transition-cation-containing clusters, however, the natural charge of the divalent cations is the predominant factor.

Binding Energy. Binding energy of a system is usually used to be a criterion for the ability of the metal ions combining with the ligands. The binding energy of the $[M_2Al(OH_2)_9(OH)_4]^{3+}$

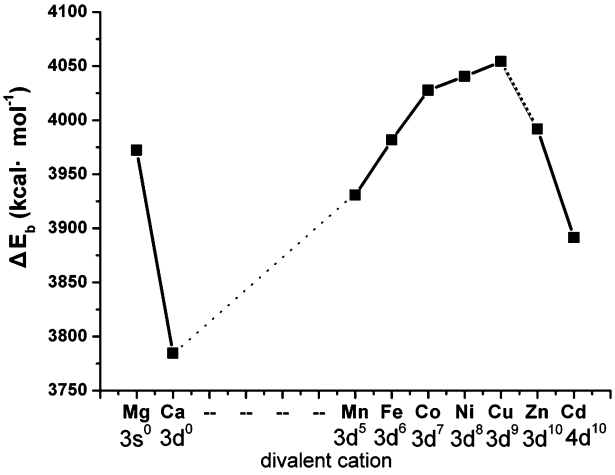

Figure 6. Relationship between zero-point corrected binding energy (ZPE) ΔE_b of the $[M_2Al(OH_2)_9(OH)_4]^{3+}$ (M = divalent metal cation) clusters and the atomic number of M^{2+}.

clusters, which corresponds to a gas-phase reaction at 0 K, can be obtained based on the equation

$$\Delta E_b = 2E_{M^{2+}} + E_{Al^{3+}} + 9E_{H_2O} + 4E_{OH^-} - E_{[M_2Al(OH_2)_9(OH)_4]^{3+}} \quad (2)$$

where ΔE_b denotes the total binding energy; $E_{M^{2+}}$ and $E_{Al^{3+}}$ denote the calculated total energy of the ground state M^{2+} and Al^{3+} ion; $E_{H_2O} = -76.4090$ au; $E_{H_2O}(ZPE) = -76.3878$ au computed with 6-31G(d) basis sets (1 au = 627.51 kcal·mol^{-1}); and $E_{[M_2Al(OH_2)_9(OH)_4]^{3+}}$ represents the total energy of the $[M_2Al(OH_2)_9(OH)_4]^{3+}$ cluster. The binding energies listed in Table 2 were corrected by zero-point energy (ZPE) (the detailed results of each term in eq 2 are given in Supporting Information, Table S2).

The binding energy of the studied clusters as a function of the atomic number of M^{2+} is plotted in Figure 6. In principle, the correlation is opposite to that of the M−O length discussed above (Figure 2A), with the difference that the maximum of the binding energy was obtained for the 2Cu−Al cluster rather than the 2Ni−Al one. This trend is consistent with the lattice energy of the metal hydroxide[17] and metallic halogenides.[18] Since in the case of Cu^{2+} an additional stabilization from Jahn−Teller distortion arises for octahedral coordination, as a result the ligand field stabilization contributions cannot be used directly for the more accurate consideration of the d^9 complex. The particular behavior of the 2Cu−Al cluster is in accordance with the experimental findings that $Cu(OH)_2$ crystallizes in a different structure type with distorted octahedral coordination around Cu^{2+} ions[17] and that Cu^{2+}-containing LDHs show a corrugation of the sheets or being diluted by other cations.[11]

Moreover, the plot of the binding energy of the studied clusters against the atomic number of M^{2+} implies the influence of the electronic structure of the divalent cation on the relative stability of the corresponding cluster. The binding energies of the clusters including both the main and 2B group closed-shell cations (Mg^{2+}, Ca^{2+}, Zn^{2+}, and Cd^{2+}) decrease with the increase of the period number (Figure 6). This indicates the higher stability of the 2Mg−Al and 2Zn−Al clusters than that of the 2Ca−Al and 2Cd−Al ones, which agrees well with the experimental results that Mg−Al and Zn−Al LDHs are the most commonly natural and synthesized LDHs.[1,34] As for Ca^{2+} and Cd^{2+} with much larger ionic radius than that of Mg^{2+}, they have also been reported to be incorporated into LDH layers to form a stable structure.[30i,35] Our previous work[16] showed that their 7-fold coordination is more stable than 6-fold coordination. This fact is not only due to their large size but also due to a less rigid structure of the 7-fold coordination in which the most stable angles could be more easily reached.

On the other hand, in the cases of the clusters including open-shelled transition cations (Mn^{2+}, Fe^{2+}, Co^{2+}, Ni^{2+}, and Cu^{2+}), the binding energy increases upon increasing the number of their 3d-electrons, as shown in Figure 6. The particular behavior of the 2Cu−Al cluster has been explained above. Therefore, the 2Ni−Al cluster should be the most stable regular brucite-like structure. This is consistent with the fact that Ni^{2+} is easy to be introduced into the LDH layers,[10] and Ni−Al hydrotalcite, called takovite, is a pyroaurite-like mineral related to hydrotalcite.[36] Moreover, the binding energies of other trasition-divalent-containing clusters increase in the order $Mn^{2+} < Fe^{2+} < Co^{2+}$, which is also in accordance with the experimental results. In fact, LDHs containing Mn^{2+} as the only divalent component in the brucite-like layer are unusual due to its redox property. The existence of "desautelsite", a naturally occurring Mg−Mn−LDH, was described by Dunn et al.[37a] The studies of synthesized binary and ternary LDHs containing manganese show that most of the Mn^{2+} were oxidized to Mn^{3+} during the synthesis process.[37b−d] Experimentally, Fe^{2+} and Co^{2+} are also difficult to be introduced into LDH layers as the only divalent component because the large octahedral CFSE of high spin d^5 of Fe^{3+} and low spin d^6 configuration of Co^{3+} facilitate the easy oxidation of Fe^{2+} to Fe^{3+} and Co^{2+} to Co^{3+}. As a result, three-component LDHs containing one element with different valence such as Co−Fe^{2+}−Fe^{3+} LDH and Mg−Co^{2+}−Co^{3+} LDH have been reported by controlling preparation conditions.[38] More recently, monometallic Fe^{2+}−Fe^{3+} LDH (green rust)[39a] and Co^{2+}−Co^{3+} LDH[39b] have been successfully prepared, and Co^{2+}−Fe^{3+} binary LDH has also been synthesized by an innovative topochemical approach.[39c] Furthermore, with the development of a synthesis technique, the binary-component M^{2+}−Al and ternary-component M^{2+}−M'^{2+}−Al LDHs (M^{2+} and M'^{2+} = Fe, Co, Ni, or Zn) with high crystalline have been reported to be prepared by the urea method under optimized conditions.[40]

As a result, the calculated binding energies of the studied clusters are in accordance with the relative stability of the corresponding cation-containing LDHs observed by experimental results.

Conclusions

A series of density functional calculations for the $[M_2Al(OH_2)_9(OH)_4]^{3+}$ clusters (M = divalent cation: closed-shelled Mg^{2+}, Ca^{2+}, Zn^{2+}, or Cd^{2+} and open-shelled Mn^{2+}, Fe^{2+}, Co^{2+}, Ni^{2+}, or Cu^{2+}, respectively) were performed at the DFT/B3LYP level, for the purpose of understanding the structural properties and relative stability of M(II)−Al binary LDH layers with the M^{2+}/Al^{3+} ratio of 2.

The cluster model presented in this work includes the basic information of the LDHs lattice structure with the most economical size and succeeds in exhibiting influences of the electronic structure of the divalent cation on the properties and stability of the corresponding LDHs. The geometric parameters (bond distance and bond angle), stretching vibration frequencies of three-centered bridging OH groups, and binding energy of the clusters were systematically discussed. Moreover, the valence electronic configuration of metal ions, Jahn−Teller effects, and natural bond orbitals (NBO) which influence the structural properties and relative stability of LDHs have also been investigated.

It was found that the geometries and stretching vibration frequencies of three-centered bridging OH groups for the calculated clusters are closely related to the different electronic structure of the divalent cations, such as valence electronic configuration, natural bond orbitals, natural charge transfer, and bond order. The calculated binding energies are in accordance with the relative stability of the corresponding LDHs obtained by experimental results. The calculation results reveal that the 2Ni−Al cluster is the most stable one among the open-shelled cation-containing clusters, while the stability of the 2Cu−Al cluster is the weakest. This can explain the experimental findings that Ni^{2+} is easy to be introduced into LDH layers,[10] whereas the Cu^{2+}-containing LDHs show a corrugation of the sheets or being diluted by other cations,[11] although both Ni^{2+} and Cu^{2+} have very close ionic radii to that of Mg^{2+}. For the closed-shelled cation-containing clusters, the 2Mg−Al and 2Zn−Al clusters are the most stable ones, which is also consistent with the experimental results.[1]

In conclusion, the electronic structure of different divalent cations plays a more significant role in the structural properties and relative stability of the corresponding LDHs rather than the ionic radius, on the basis of our DFT theoretical calculation results. This work provides important and accurate insight into the construction rules for LDH materials beyond the previously ambiguous understanding and gives a clear hint for the design and preparation of LDHs and related materials with prospective applications.

Acknowledgment. This work was supported by the National Natural Science Foundation of China, the Program for New Century Excellent Talents in University (Grant No.: NCET-05-121), the 111 Project (Grant No.: B07004), the 973 Program (Grant No.:2009CB939802), and the Program for Changjiang Scholars and Innovative Research Team in University (Grant No.: IRT0406).

Supporting Information Available: The optimized geometries of $[M_2Al(OH_2)_9(OH)_4]^{3+}$ (M = divalent cation Mg^{2+}, Ca^{2+}, Mn^{2+}, Fe^{2+}, Co^{2+}, Ni^{2+}, Cu^{2+}, Zn^{2+}, or Cd^{2+}) clusters (Figure S1); calculated NBO parameters of the optimized clusters (Table S1); total energies, zero-point corrected total energies, and the frequency minima of the optimized clusters (Table S2); and Cartesian coordinates of optimized cluster models (Table S3). This material is available free of charge via the Internet at http://pubs.acs.org.

References and Notes

(1) (a) Cavani, F.; Trifirò, F.; Vaccari, A. *Catal. Today* **1991**, *11*, 173. (b) Vaccari, A. *Appl. Clay Sci.* **1999**, *14*, 161.

(2) (a) Williams, G. R.; O'Hare, D. *J. Mater. Chem.* **2006**, *16*, 3065. (b) Rives, V.; Ulibarri, M. A. *Coord. Chem. Rev.* **1999**, *181*, 61. (c) Khan, A. I.; O'Hare, D. *J. Mater. Chem.* **2002**, *12*, 3191.

(3) Duan, X.; Evans, D. G., Eds. *Layered Double Hydroxides, Structure and Bonding*; Springer: Berlin/Heidelberg, 2006; Vol. 119.

(4) Newman, S. P.; Greenwell, H. C.; Coveney, P. V.; Jones, W. *Layered Double Hydroxides: Present and Future*; Nova Science: New York, 2001; p 1.

(5) (a) Tichit, D.; Ribet, S.; Coq, B. *Eur. J. Inorg. Chem.* **2001**, 539. (b) Xu, Z.; Zeng, H. *Chem. Mater.* **2001**, *13*, 4555. (c) Rives, V.; Dubey, A.; Kannan, S. *Phys. Chem. Chem. Phys.* **2001**, *3*, 4826. (d) Rojas, R. M.; Kovacheva, D.; Petrov, K. *Chem. Mater.* **1999**, *11*, 3263. (e) Velu, S.; Suzuki, K.; Hashimoto, S.; Satoh, N.; Ohashi, F.; Tomura, S. *J. Mater. Chem.* **2001**, *11*, 2049.

(6) (a) Hou, X.; Kalinichev, A. G.; Kirkpatrick, R. J. *Chem. Mater.* **2002**, *14*, 2078. (b) Fogg, A. M.; Freij, A. J.; Parkinson, G. M. *Chem. Mater.* **2002**, *14*, 232. (c) Fogg, A. M.; Dunn, J. S.; O'Hare, D. *Chem. Mater.* **1998**, *10*, 356.

(7) (a) Shu, X.; Zhang, W.; He, J.; Gao, F.; Zhu, Y. *Solid State Sci.* **2006**, *8*, 634. (b) Velu, S.; Ramaswamy, V.; Ramani, A.; Chanda, B. M.; Sivasanker, S. *Chem. Commun.* **1997**, 2107. (c) Velu, S.; Suzuki, K.; Okazaki, M.; Osaki, T.; Tomura, S.; Ohashi, F. *Chem. Mater.* **1999**, *11*, 2163. (d) Intissar, M.; Jumas, J. C.; Besse, J. P.; Leroux, F. *Chem. Mater.* **2003**, *15*, 4625.

(8) (a) Sels, B. F.; De Vos, D. E.; Jacobs, P. A. *Angew. Chem., Int. Ed.* **2005**, *44*, 310. (b) Choy, J. H.; Kwak, S. Y.; Park, J. S.; Jeong, Y. J.; Portier, J. *J. Am. Chem. Soc.* **1999**, *121*, 1399. (c) Itoh, T.; Shichi, T.; Yui, T.; Takahashi, H.; Inui, Y.; Takagi, K. *J. Phys. Chem. B* **2005**, *109*, 3199. (d) Gursky, J. A.; Blough, S. D.; Luna, C.; Gomez, C.; Luevano, A. N.; Gardner, E. A. *J. Am. Chem. Soc.* **2006**, *128*, 8376. (e) Mohanambe, L.; Vasudevan, S. *J. Phys. Chem. B* **2005**, *109*, 15651. (f) Liu, Z.; Ma, R.; Osada, M.; Iyi, N.; Ebina, Y.; Takada, K.; Sasaki, T. *J. Am. Chem. Soc.* **2006**, *128*, 4872. (g) Chen, H.; Zhang, F.; Fu, S.; Duan, X. *Adv. Mater.* **2006**, *18*, 3089. (h) Lee, J. H.; Rhee, S.; Jung, D. Y. *J. Am. Chem. Soc.* **2007**, *129*, 3522. (i) Zhang, F.; Zhao, L.; Chen, H.; Xu, S.; Evans, D. G.; Duan, X. *Angew. Chem., Int. Ed.* **2008**, *47*, 2466.

(9) Shannon, R. D. *Acta Crystallogr.* **1976**, *A32*, 751.

(10) (a) Tichit, D.; Durand, R.; Rolland, A.; Coq, B.; Lopez, J.; Marion, P. *J. Catal.* **2002**, *211*, 511. (b) Beres, A.; Palinko, I.; Kiricsi, I.; Mizukami, F. *Solid State Ionics* **2001**, *141−142*, 259. (c) Takehiraa, K.; Shishidob, T.; Shouroc, D.; Murakamia, K.; Hondac, M.; Kawabataa, T.; Takakia, K. *Appl. Catal. A: Gen.* **2005**, *279*, 41. (d) Gérardin, C.; Kostadinova, D.; Coq, B.; Tichit, D. *Chem. Mater.* **2008**, *20*, 2086. (e) Han, Y.; Liu, Z. H.; Yang, Z.; Wang, Z.; Tang, X.; Wang, T.; Fan, L.; Ooi, K. *Chem. Mater.* **2008**, *20*, 360.

(11) (a) Alejandre, A.; Medina, F.; Salagre, P.; Correig, X.; Sueiras, J. E. *Chem. Mater.* **1999**, *11*, 939. (b) Roussel, H.; Briois, V.; Elka, M. E.; de Roy, A.; Besse, J. P. *J. Phys. Chem. B* **2000**, *104*, 5915. (c) Bigey, L.; Depège, C.; de Roy, A.; Besse, J. P. *J. Physique IV* **1997**, *7*, C2−949. (d) Feng, Y.; Li, D.; Li, C.; Wang, Z.; Evans, D. G.; Duan, X. *Clay Clay Miner.* **2003**, *51*, 566.

(12) (a) Greenwell, H. C.; Jones, W.; Coveney, P. V.; Stackhouse, S. *J. Mater. Chem.* **2006**, *16*, 708. (b) Lombardo, G. M.; Pappalardo, G. C.; Punzo, F.; Costantino, F.; Costantino, U.; Sisani, M. *Eur. J. Inorg. Chem.* **2005**, 5026. (c) Mohanambe, L.; Vasudevan, S. *J. Phys. Chem. B* **2005**, *109*, 15651. (d) Kalinichev, A. G.; Kirkpatrick, R. J. *Chem. Mater.* **2002**, *14*, 3539. (e) Greenwell, H. C.; Jones, W.; Newman, S. P.; Coveney, P. V. *J. Mol. Struct.* **2003**, *647*, 75. (f) Mohanambe, L.; Vasudevan, S. *Langmuir* **2005**, *21*, 10735. (g) Kumar, P. P.; Kalinichev, A. G.; Kirkpatrick, R. J. *J. Phys. Chem. B* **2006**, *110*, 3841. (h) Newman, S. P.; Williams, S. J.; Coveney, P. V.; Jones, W. *J. Phys. Chem. B* **1998**, *102*, 6710. (i) Wang, J. W.; Kalinichev, A. G.; Kirkpatrick, R. J.; Hou, X. *Chem. Mater.* **2001**, *13*, 145. (j) Cygan, R. T.; Liang, J. J.; Kalinichev, A. G. *J. Phys. Chem. B* **2004**, *108*, 1255. (k) Aicken, A. M.; Bell, I. S.; Coveney, P. V.; Jones, W. *Adv. Mater.* **1997**, *9*, 409. (l) Li, H.; Ma, J.; Evans, D. G.; Zhou, T.; Li, F.; Duan, X. *Chem. Mater.* **2006**, *18*, 4405. (m) Thyveetil, M. A.; Coveney, P. V.; Greenwell, H. C.; Suter, J. L. *J. Am. Chem. Soc.* **2008**, *130*, 4742.

(13) (a) Stackhouse, S.; Coveney, P. V.; Sandre, E. *J. Am. Chem. Soc.* **2001**, *123*, 11764. (b) Greenwell, H. C.; Stackhouse, S.; Coveney, P. V.; Jones, W. *J. Phys. Chem. B* **2003**, *107*, 3476. (c) Refson, K.; Park, S. H.; Sposito, G. *J. Phys. Chem. B* **2003**, *107*, 13376. (d) Trave, A.; Selloni, A.; Goursot, A.; Tichit, D.; Weber, J. *J. Phys. Chem. B* **2002**, *106*, 12291.

(14) Gorb, L. G.; Aksenenko, E. V.; Adams, J. W.; Larson, S. W.; Weiss, C. A.; Leszczynska, D.; Leszczynski, J. *J. Mol. Struct.* **1998**, *425*, 129.

(15) (a) Peterson, R. C.; Hill, R. J.; Gibbss, G. V. *Can. Mineral.* **1979**, *17*, 703. (b) Pu, M.; Zhang, B. *Mater. Lett.* **2005**, *59*, 3343. (c) Sato, H.; Morita, A.; Ono, K.; Nakano, H.; Wakabayashi, N.; Yamagishi, A. *Langmuir* **2003**, *19*, 7120. (d) Sainz-Diaz, C. I.; Timon, V.; Botella, V.; Hernandez-Laguna, A. *Am. Mineral.* **2000**, *85*, 1038.

(16) Yan, H.; Lu, J.; Wei, M.; Ma, J.; Li, H.; He, J.; Evans, D. G.; Duan, X. *J. Mol. Struct.- THEOCHEM* **2008**, *866*, 34.

(17) Oswald, H. R.; Asper, R. Bivalent metal hydroxides. *Preparation and Crystal Growth of Materials with Layered Structures*; Lieth, R. M. A., Ed.; Reidel Pub Co: Holland, 1977; p 71.

(18) Schläfer, H. L.; Gliemann, G. *Basical Principles of Ligand Field Theory*; John Wiley & Sons Ltd., 1969; p 142.

(19) (a) Becke, A. D. *Phys. Rev. A* **1988**, *38*, 3098. (b) Lee, C.; Yang, W.; Parr, R. G. *Phys. Rev. B* **1988**, *37*, 785. (c) Vosko, S. H.; Wilk, L.; Nussair, M. *Can. J. Phys.* **1980**, *58*, 1200. (d) Becke, A. D. *J. Chem. Phys.* **1993**, *98*, 5648.

(20) (a) Hay, P. J.; Wadt, W. R. *J. Chem. Phys.* **1985**, *82*, 270. (b) Wadt, W. R.; Hay, P. J. *J. Chem. Phys.* **1985**, *82*, 284. (c) Hay, P. J.; Wadt, W. R. *J. Chem. Phys.* **1985**, *82*, 299.

(21) Petersson, G. A.; Al-Laham, M. A. *J. Chem. Phys.* **1991**, *94*, 6081.

(22) Frisch, M. J.; Trucks, G. W.; Schlegel, H. B.; Scuseria, G. E.; Robb, M. A.; Cheeseman, J. R.; Montgomery, J. A.; Vreven, T., Jr.; Kudin, K. N.; Burant, J. C.; Millam, J. M.; Iyengar, S. S.; Tomasi, J.; Barone, V.; Mennucci, B.; Cossi, M.; Scalmani, G.; Rega, N.; Petersson, G. A.; Nakatsuji, H.; Hada, M.; Ehara, M.; Toyota, K.; Fukuda, R.; Hasegawa, J.; Ishida, M.; Nakajima, T.; Honda, Y.; Kitao, O.; Nakai, H.; Klene, M.; Li, X.; Knox, J. E.; Hratchian, H. P.; Cross, J. B.; Adamo, C.; Jaramillo, J.; Gomperts, R.; Stratmann, R. E.; Yazyev, O.; Austin, A. J.; Cammi, R.; Pomelli, C.; Ochterski, J. W.; Ayala, P. Y.; Morokuma, K.; Voth, G. A.;

Salvador, P.; Dannenberg, J. J.; Zakrzewski, V. G.; Dapprich, S.; Daniels, A. D.; Strain, M. C.; Farkas, O.; Malick, D. K.; Rabuck, A. D.; Raghavachari, K.; Foresman, J. B.; Ortiz, J. V.; Cui, Q.; Baboul, A. G.; Clifford, S.; Cioslowski, J.; Stefanov, B. B.; Liu, G.; Liashenko, A.; Piskorz, P.; Komaromi, I.; Martin, R. L.; Fox, D. J.; Keith, T.; Al-Laham, M. A.; Peng, C. Y.; Nanayakkara, A.; Challacombe, M.; Gill, P. M. W.; Johnson, B.; Chen, W.; Wong, M. W.; Gonzalez, C.; Pople, J. A. *Gaussian 03*, revision B.04; Gaussian, Inc.: Pittsburgh, PA.

(23) Rauhut, G.; Pulay, P. *J. Phys. Chem.* **1995**, *99*, 3093.

(24) (a) Reed, A. E.; Curtiss, L. A.; Weinhold, F. *Chem. Rev.* **1988**, *88*, 899. (b) Foster, J. P.; Weinhold, F. *J. Am. Chem. Soc.* **1980**, *102*, 7211.

(25) (a) Glendening, E. D.; Reed, A. E.; Carpenter, J. E.; Weinholk, F. *NBO*, version 3.1. (b) Glendening, E. D.; Badenhoop, J. K.; Reed, A. E.; Carpenter, J. E.; Bohmann, J. A.; Morales, C. M.; Weinhold, F. *NBO*, version 5.0.

(26) (a) Arakcheeva, A. V.; Pushcharovskii, D. Y.; Rastsvetaeva, R. K. *Z. Kristallogr.* **1996**, *41*, 1024. (b) Bellotto, M.; Rebours, B.; Clause, O.; Lynch, J.; Bazin, D.; Elkaim, E. *J. Phys. Chem.* **1996**, *100*, 8527. (c) Zigan, F.; Rothbauer, R. *Neues. Jahrb. Mineral. Monatsh.* **1967**, *4*−*5*, 245. (d) Terzis, A.; Filippakis, S.; Kuzl, J.; Burzhaff, H. *Z. Kristallogr.* **1987**, *181*, 29. (e) Petch, H. E. *Acta Crystallogr.* **1961**, *14*, 950. (f) Norlund Christensen, A.; Ollivier, G. *Solid State Commun.* **1972**, *10*, 609. (g) Penfold, B. R.; Taylor, M. R. *Acta Crystallogr.* **1960**, *13*, 953. (h) Thompson, H. A.; Parks, G. A.; Brown, G. E., Jr. *Geochim. Cosmochim. Acta* **1999**, *63*, 1767. (i) Lotmar, W.; Feitknecht, W. *Z. Kristallogr.* **1936**, *93*, 368. (j) Cairns, R. W.; Ott, E. *J. Am. Chem. Soc.* **1933**, *55*, 527. (k) Oswald, H. R.; Reller, A.; Schmalle, H. W.; Dubler, E. *Acta Crystallogr. C* **1990**, *46*, 2279. (l) Baneeva, M. I.; Popova, S. V. *Geokhimiya* **1969**, 1014. (m) Ennadi, A.; Legrouri, A.; Roy, A. D.; Besse, J. P. *J. Solid State Chem.* **2000**, *152*, 568. (n) Bertrand, G.; Dusausoy, Y. *Sci. Chim.* **1970**, *270*, 612. (o) Saalfeld, H.; Wedde, M. *Z. Kristallogr.* **1973**, *139*, 9.

(27) Catti, M.; Ferraris, G.; Hull, S.; Pavese, A. *Phys. Chem. Miner.* **1995**, *22*, 200.

(28) Frenking, G.; Fröhlich, N. *Chem. Rev.* **2000**, *100*, 717.

(29) Kallies, B.; Meier, R. *Inorg. Chem.* **2001**, *40*, 3101.

(30) (a) Hemandez-Moreno, M. J. H.; Ulibarri, M. A.; Rendon, J. L.; Sema, C. J. *Phys. Chem. Miner.* **1985**, *12*, 34. (b) Brindley, G. W.; Kao, C. C. *Phys. Chem. Miner.* **1984**, *10*, 187. (c) Raki, L.; Beaudoin, J. J.; Mitchell, L. *Cem. Concr. Res.* **2004**, *34*, 1717. (d) Aisawa, S.; Hirahara, H.; Uchiyama, H.; Takahashi, S.; Narita, E. *J. Solid State Chem.* **2002**, *167*, 152. (e) Kannan, S.; Swamy, C. S. *J. Mater. Sci.* **1997**, *32*, 1623. (f) Jitianu, M.; Balasoiu, M.; Marchidan, R.; Zaharescu, M.; Crisan, D.; Craiu, M. *Int. J. Inorg. Mater.* **2000**, *2*, 287. (g) Rives, V.; Dubey, A.; Kannan, S. *Phys. Chem. Chem. Phys.* **2001**, *3*, 4826. (h) Velu, S.; Ramkumar, V.; Narayanan, A.; Swamy, C. S. *J. Mater. Sci.* **1997**, *32*, 957. (i) Vivhi, F. M.; Alves, O. L. *J. Mater. Chem.* **1997**, *7*, 1631.

(31) Vedder, W. *Am. Mineral.* **1964**, *49*, 736.

(32) Robort, J. L.; Kodama, H. *Am. J. Sci.* **1988**, *288A*, 196.

(33) Besson, G.; Drits, V. A. *Clay Clay Miner.* **1997**, *45*, 170.

(34) (a) Velu, S.; Ramkumar, V.; Narayanan, A.; Swamy, C. S. *J. Mater. Sci.* **1997**, *32*, 957. (b) Ennadi, A.; Legrouri, A.; Roy, A. D.; Besse, J. P. *J. Solid State Chem.* **2000**, *152*, 568. (c) Chang, Z.; Evans, D. G.; Duan, X.; Vial, C.; Ghanbaja, J.; Prevot, V.; Roy, M. D.; Forano, C. *J. Solid State Chem.* **2005**, *178*, 2766. (d) Hussein, M. Z.; Hwa, T. K. *J. Nanopart. Res.* **2000**, *2*, 293. (e) Liu, J.; Huang, X.; Li, Y.; Sulieman, K. M.; He, X.; Sun, F. *J. Phys. Chem. B* **2006**, *110*, 21865.

(35) Guo, Y.; Zhang, H.; Zhao, L.; Li, G.; Chen, J.; Xu, L. *J. Solid State Chem.* **2005**, *178*, 1830.

(36) (a) Allmann, R. *Acta Crystallogr. B* **1968**, *24*, 972. (b) Taylor, H. F. W. *Mineral. Mag.* **1973**, *39*, 377.

(37) (a) Dunn, P. J.; Peacot, D. R.; Palmer, T. D. *Am. Mineral.* **1979**, *64*, 127. (b) Hansen, H. C. B.; Taylor, R. M. *Clay Miner.* **1991**, *26*, 507. (c) Fernandez, J. M.; Barriga, C.; Ulibarri, M. A.; Labajos, F. M.; Rives, V. *J. Mater. Chem.* **1994**, *4*, 1117. (d) Velu, S.; Shah, N.; Jyothi, T. M.; Sivasanker, S. *Microporous Mesoporous Mater.* **1999**, *33*, 61.

(38) (a) Liu, J.; Li, F.; Evans, D. G.; Duan, X. *Chem. Commun.* **2003**, 542. (b) Radha, A. V.; Thomas, G. S.; Kamath, P. V.; Shivakumara, C. *J. Phys. Chem. B* **2007**, *111*, 3384. (c) Xu, Z.; Zeng, H. *J. Mater. Chem.* **1998**, *8*, 2499. (d) Sampanthar, J. T.; Zeng, H. *Chem. Mater.* **2001**, *13*, 4722.

(39) (a) Simon, L.; François, M.; Refait, P.; Renaudin, G.; Lelaurain, M.; Génin, J. M. R. *Solid State Sci.* **2003**, *5*, 327. (b) Ma, R.; Takada, K.; Fukuda, K.; Iyi, N.; Bando, Y.; Sasaki, T. *Angew. Chem., Int. Ed.* **2008**, *47*, 86. (c) Ma, R.; Liu, Z.; Takada, K.; Iyi, N.; Bando, Y.; Sasaki, T. *J. Am. Chem. Soc.* **2007**, *129*, 5257.

(40) (a) Ma, R.; Liu, Z.; Li, L.; Iyi, N.; Sasaki, T. *J. Mater. Chem.* **2006**, *16*, 3809. (b) Liu, Z.; Ma, R.; Ebina, Y.; Iyi, N.; Nobuo, I.; Takada, K.; Sasaki, T. *Langmuir* **2007**, *23*, 861.

JP810129H